Carbohydrate Polymers 83 (2011) 512–519

Contents lists available at ScienceDirect

Carbohydrate Polymers

journal homepage: www.elsevier.com/locate/carbpol

# Surface-initiated atom transfer radical polymerization of butyl acrylate on cellulose microfibrils

Miaomiao Xiao[a], Shuzhao Li[a,b], Wilailak Chanklin[a], Anna Zheng[b], Huining Xiao[a,*]

[a] Department of Chemical Engineering, University of New Brunswick, Fredericton, NB E3B 5A3, Canada
[b] School of Materials Science & Engineering, East China University of Science & Technology, Shanghai 200237, China

ARTICLE INFO

*Article history:*
Received 21 April 2010
Received in revised form 5 August 2010
Accepted 9 August 2010
Available online 14 August 2010

*Keywords:*
Cellulose microfibril (CMF)
SI-ATRP
Macroinitiator
Butyl acrylate
Grafting

ABSTRACT

Surface-initiated atom transfer radical polymerization (SI-ATRP) of butyl acrylate (BA) on cellulose microfibrils (CMF) was conducted to create controllable hydrophobic chains on CMF. The macroinitiator, CMF-Br, was prepared by the esterification of hydroxyl groups on CMF with 2-bromoisobutyrylbromide (BIBB); followed by the ATRP of BA using two catalyst systems, $Cu^{I}Br$/2,2′-bipyridine (BPY) and $Cu^{I}Br$/pentamethyl-diethylenetriamine (PMDETA). The molecular weight (MW) and polydispersity of the grafted PBA cleaved from CMF via hydrolysis was determined using GPC. The results indicated that the PMDETA system exhibited relatively poor control over the ATRP; whereas the BPY system produced the PBA with tailored chain lengths and relatively narrow polydispersities but experienced a rather slow polymerization process. To optimize the polymerization with the CuBr/PMDETA system, several influencing factors were investigated, including the type of solvents, reaction temperature and the use of co-catalyst $Cu^{II}Br_2$. The hydrophobic-modified CMF is of great potential as reinforcements biocomposites.



## 1. Introduction

Biocomposites or nanocomposites based on cellulose microfibrils (CMF) attract strong interest because of the combination of properties of the biomaterials (mechanical, biodegradable, inexpensive, and renewable) and the polymer (higher melt point, chemical resistance, low density and plasticity) (Amash & Zugenmaier, 1998; Dufresne, Cavaille, & Helbert, 1996; Mohamed, Mostafa, & Alain, 2005; Otto van den, Michael, Jeffrey, & Christoph, 2007; William et al., 2005). However, the exploitation of these properties requires the nano-particles well-dispersed in the polymer matrices. Unfortunately, CMF cannot develop its reinforcement capacity in polymer composites because of the poor adhesion to common non-polar matrices, such as polypropylene. This is mainly attributed to the high polarity and hydrophilicity of CMF. The poor compatibility causes agglomeration of CMF and weakens the interaction with polymer matrices, which induces a reduction of mechanical properties (Belgacem & Gandini, 2005). One of the approaches to enhance the interaction is to render the surface of CMF hydrophobic via grafting, thus improving various physical and chemical properties; including the heat resistance, elasticity, ion-exchange capabilities, resistance to abrasion and wear, oil and water repellency, and antibacterial activity (Gupta & Sahoo, 2001; Vigo, 1998). Of these modifications, the grafting of hydrophobic polymers, such as methyl methacrylate, styrene, acrylonitrile, and butyl acrylate, onto cellulose strengthens the CMF adhesion to hydrophobic polymers significantly (Zhang & Chen, 2002), which is crucial when cellulose fibers are used as reinforcements in composites (Carlmark & Malmstrom, 2003).

The surface of cellulose fibers have been modified by graft polymerizations via various methods in the past (Castellano, Gandini, Fabbri, & Belgacem, 2004; Favier, Chanzy, & Cavaille, 1995; Kalaprasad & Alain, 2003; Uchida & Ikada, 1997; Zadorecki & Ronnhult, 1986). Most of them are based on "grafting onto" and "grafting from" techniques. For the "grafting onto" method, strong hindrance between grafted polymer chains prevents attachment of further ones and then limits the graft density (Carlmark & Malmstrom, 2003). In "grafting from" method, chain scission can occur and does not necessarily render the cellulose backbone intact (Koening & Roberts, 1974). Also it is impossible for these methods to predetermine the length of each pendent chain or arm and the molecular weight distribution. The surface-initiated atom transfer radical polymerization (SI-ATRP) technique has attracted intensive interest for the surface grafting high-density polymer with the controllable molecular weight, molecular weight distribution, and well-defined structure (Liu & Guo, 2006; Pyun, Kowalewski, & Matyjaszewski, 2003). Furthermore, almost all the polymers formed were chemical-bonded onto the matrices and no non-grafted polymers were obtained in the SI-ATRP process. Up to now, the SI-ATRP technique has been successfully employed to graft

* Corresponding author. Tel.: +1 506 453 3532; fax: +1 506 453 3591.
*E-mail address:* hxiao@unb.ca (H. Xiao).

0144-8617/$ – see front matter © 2010 Elsevier Ltd. All rights reserved.
doi:10.1016/j.carbpol.2010.08.011

polymers to various surfaces such as silicon (Matyjaszewski, Miller, Shukla, & Immarporn, 1999; Zhao & Brittain, 1999), silica (Shah et al., 2000), gold (Li, He, Cui, & Li, 2007), magnetite (Marutani et al., 2004) and porous substrates (Ejaz, Tsujii, & Fukuda, 2001). Furthermore, SI-ATRP has also been used to graft polymers onto cellulose fiber (David, Katja, Helge, & Søren, 2005; Glaied, Dubé, Chabot, & Daneault, 2009; Josefina et al., 2008; Valter, Marco, Simone, & Giulia, 2007; Zampano, Bertoldo, Bronco, & Simona, 2009), macroscopic cellulose fibers (Anna & Eva, 2003; Josefina & Eva, 2006; Plackett, Jankova, Egsgaard, & Hvilsted, 2005; Robert, Anna, Anders, Eva, & Isabel, 2007; Sang & Xiao, 2009), cellulose powder (Coskun & Temüz, 2005) and cellulose nanocrystals (Gaelle, Lindy, & Wim, 2009; Singh et al., 2008). For instance, the surface-initiated ATRP of acrylamide was conducted on silica at room temperature by using a catalyst system of $CuCl/CuCl_2$/tris(2-dimethyl-aminoethyl)-amine (Xiao & Wirth, 2002). It was found that the thickness of the polyacrylamide film is proportional to the monomer concentration but not to reaction time. Carrot, Diamanti, Manuszak, Charleux, & Vairon (2001) reported the silica enanocomposites with a hard core and a soft shell using SI-ATRP of butyl acrylate. Kong, Tadashi, Jiro, and Tomokazu (2001) successfully prepared homopolymer and block amphiphilic brush on silicon wafers by combining the self-assembled monolayer of initiator and ATRP. The amphiphilic block copolymer brushes consisting of PAAM and PMMA blocks were obtained by using the homopolymer bush as a macroinitiator for the follow-up ATRP polymerization of the second monomer. To our knowledge, few studies have been performed on the surface of cellulose fibers via SI-ATRP.

In this work, the SI-ATRP of butyl acrylate (BA) onto CMF was conducted in an attempt to render CMF hydrophobic. The resulting hydrophobic-modified CMF could be further used as reinforcement for polymer, polypropylene (PP) in particular, to generate biocomposites which are of interest for automobile application. Compared with cellulose fibers, CMF appears to be much smaller. The relatively large specific areas are expected to facilitate the graft polymerization for surface modification. In the current work, the selection of butyl acrylate for SI-ATRP is based on the fact that PBA on CMF surfaces would not only improve the compatibility between CMF with polymer matrix of PBA, but also act as elastomeric interfacial layer which is of great, potential in improving the impact strength of the resulting biocomposites. To maximize the performance of the PBA-modified CMF, various influencing factors, such as polymerization conditions, the choice of ligand and solvent, and the use of deactivator have been investigated in this work in an attempt to achieve the optimal control of SI-ATRP of BA on CMF.

## 2. Experimental

### 2.1. Materials

Cellulose microfiber (CMF; mean particle size 60 μm; bulk density 0.3 g/cm$^3$), derived from cotton linters (obtained by mechanical treatment), was obtained from Aldrich. The CMF powders were dried in a vacuum oven at 60 °C for 24 h prior to use. Butyl acrylate (BA), also from Aldrich, was first washed with dilute NaOH solution to extract the polymerization inhibitor, and then washed with distilled water, followed by drying and distillation under vacuum before use. $Cu^{I}Br$ was purified by stirring it in acetic acid for 24 h, washing with methanol, and then drying. 1-methyl-2-pyrrolidinone (NMP) was purified by distillation over $CaH_2$. 2,2′-Bipyridine (BPY) from Aldrich was purified by recrystallization in cold hexane and dried in vacuum oven for 24 h. Triethylamine (TEA), 4-(dimethylamino) pyridine (DMAP), 2-bromoisobutyryl-bromide (BIBB), N,N,N′,N′,N″-pentamethyl-diethylenetriamine (PMDETA), $Cu^{II}Br_2$, toluene, 1-butanol and dimethylformamide (DMF), all from Aldrich, were used as received. Spectrum® Membranes with approximate molecular weight cut off (MWCO) at 1000 Da were used as dialysis tubes for the separation of undesired compounds or unreacted agents.

### 2.2. Synthesis of CMF-Br

To a three-necked round-bottom flask, 10 g of dried CMF particles, 250 ml of NMP solvent, 0.1 mol of TEA and 0.05 mol of DMAP were added. 50 ml of NMP solution containing 0.092 mol of BIBB was then added dropwise over 1.5 h at 0 °C after the system was degassed and backfilled with nitrogen for three cycles. The reaction proceeded under nitrogen at 0 °C for 24 h and continued at room temperature for 48 h. The resulting product, macroinitiator CMF-Br, was filtered and washed with ethanol to remove the impurities. The final product was dried at 60° in vacuum oven for 24 h.

### 2.3. General procedure for the SI-ATRP of BA

In a typical example, the polymerization of butyl acrylate was carried out under nitrogen, in a dried three-neck round-bottom flask (50 ml) equipped with a magnetic bar. CMF-Br (1 g, 0.8 mmol of Br), PMDETA (0.167 ml, 0.8mmol), $Cu^{I}Br$ (0.115 g, 0.8 mmol) 20 ml of DMF were added into the flask, which was then sealed with a rubber septum and glass stoppers. The flask contents were then cycled between vacuum and nitrogen three times to remove oxygen. Degassed butyl acrylate (4.45 ml, 31 mmol) was added using a syringe. The flask was then immersed in an oil bath heated at 90 °C. The grafting yields at different time intervals were determined by thermogravimetrical analysis (TGA) measurement of aliquots collected from the reaction mixture and purified by filtration and washing with methanol. After the reaction was complete, the reaction mixture was cooled to room temperature and the final products were purified by filtration and washing with methanol for several times to remove Cu complexes.

Grafting yield ($G_y$), the weight percent of PBA grafted on CMF based on the initial weight of CMF, was calculated according to the following equation:

$$G_y = \frac{W_{PBA}}{W_{CMF}} \quad (1)$$

where $W_{PBA}$ and $W_{CMF}$ are the weights of PBA grafted onto CMF and the total weight of grafted CMF, respectively; both were determined by TGA measurements.

### 2.4. Cleavage of PBA grafts from CMF-PBA surface

In order to investigate the molecular weight and polydispersity of PBA grafts on CMF surface, CMF-PBA samples were extracted overnight in methanolic HCl to cleave covalently bound PBA from the CMF-PBA. The fibers were then filtered off and rinsed with distilled water. The extracted solution containing the cleaved was analyzed using GPC. It is noteworthy that after hydrolyzed CMF-PBA, the linear polymer remained in the solution is poly(acrylic acid) (PAA) due to the removal of ester groups over the hydrolysis. Therefore, the molecular weight of the cleaved polymers obtained from GPC represents the MW of PAA, which is proportional to that of PBA chains.

### 2.5. Characterization

The infrared spectra of CMF-Br were recorded between 4000 and 400 cm$^{-1}$ on a Perkin-Elmer Spectrum 100 FT-IR.

Using a SDT Q600 TA instrument, the decomposition measurements based on TGA were conducted at the temperatures ranging

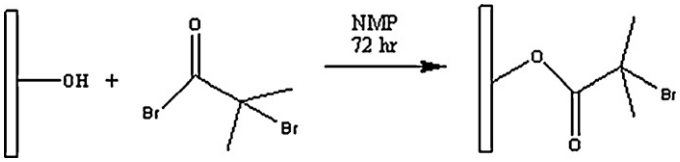


**Scheme 1.** Formation of BIBB-grafts on CMF in preparing the macroinitiator CMF-Br.

50–600 °C at a scanning rate of 20 °C/min under a helium atmosphere.

The number-average molecular weight ($M_n$) and molecular weight distribution (MWD) of the polymer cleaved from CMF-PBA (i.e., PAA) were measured on a GPCMax VE201 gel permeation chromatography (GPC) (Viscotek Co.) equipped with three columns PAA-202-204-205 and three detectors, viscometer, light scattering and IR detector. The calibration was made with poly (ethylene oxide) standards. The $M_n$ of PBA was calculated from the results of PAA.

A 300 MHz Varian Unity 400 spectrometer was used for $^1$H NMR analysis.

Energy dispersive X-ray analysis (EDAX) was measured using a Hitachi SU-70 FE-SEM equipped with an Oxford-INCA (x-act LN2-free SDD Detector) energy dispersive X-ray analyzer (accelerating voltage 15 kV).

## 3. Results and discussion

### 3.1. Characterization and quantificational determination of CMF-Br

The macroinitiator, CMF-Br, was prepared by the esterization of hydroxyl groups on the surface of the CMF with 2-bromoisobutyrylbromide (BIBB) (Scheme 1). After the surface modification of the CMF, FT-IR and EDAX were used to confirm the existence of bromine element on the surface of CMF. Fig. 1 presents the FT-IR spectra of original CMF and the purified CMF-Br. As can be seen, after the reaction, two new peaks were observed at 1738 cm$^{-1}$ and 579 cm$^{-1}$, which were attributed to the stretching vibration of carbonyl groups and C-Br groups in BIBB compound, respectively. In EDAX spectrum (Fig. 2), the Br peak was observed around 1.48 keV on the spectrum of CMF-Br, implying the formation of CMF-Br macromolecular initiators.

To control the molecular weight and polydispersity of PBA grafted on the CMF, the amount of Br on the surface of CMF-Br was quantified by TGA measurement.

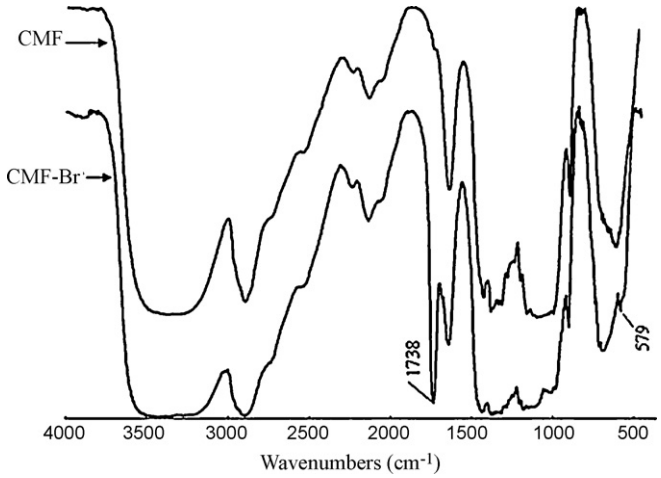


**Fig. 1.** FT-IR spectra of CMF and the purified CMF-Br.

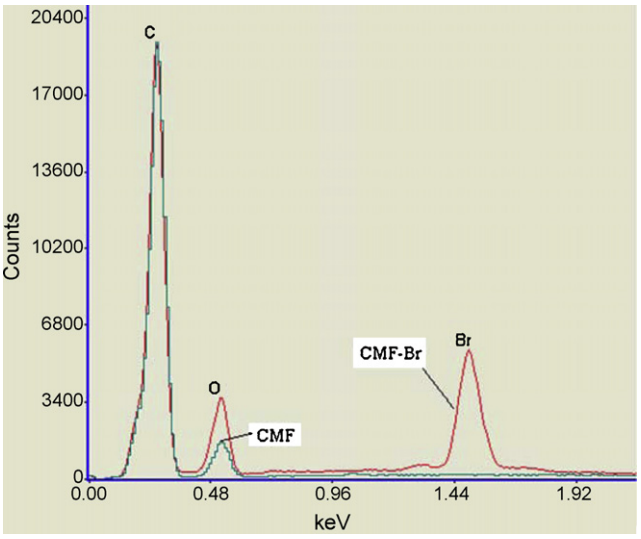


**Fig. 2.** EDAX spectra of CMF and the purified CMF-Br.

Fig. 3 shows the thermogravimetric decomposition thermograms taken between 50 and 700 °C for the CMF and CMF-Br. Clearly, only one sharp weight loss was observed for the CMF at the temperature around 317 °C, which corresponds to the onset of decomposition, $T_d$, of CMF. In contrast, the first onset of decomposition of CMF-Br was found at the temperature below 230 °C. Furthermore, CMF decomposed over a narrower temperature range, whereas the CMF-Br over a wider range. The decrease in $T_d$ and the wider range observed for the CMF-Br provided the evidence for the presence of BIBB. The initial slight weight loss resulted from the degradation of BIBB, although a degradation temperature of 250 °C for BIBB grafted on carbon nanotubes was reported (Kong, Gao, & Yan, 2004). The derivative thermogravimetry (DTG) curves shown in Fig. 3 even more clearly revealed the decomposition of CMF-Br in detail. Apparently, there are three separate degradation steps at the temperature above 100 °C, representing the decomposition of CMF-Br step by step. The shoulder decomposition peak appearing around 375 °C is indicative of the complete decomposition of CMF. Alternatively, it may also result from the thermal degradation of a new crosslinked material formed by thermal crosslinking reactions occurring in initial stages of the degradation process (Grassie & MacFarlane, 1978; Grassie, Murry, & Holmes, 1984). The maximum DTG peak at 260 °C is caused by the degradation of the CMF in CMF-Br. The decrease of $T_d$ is attributed to the substitution of hydroxyl groups on CMF with BIBB, which is con-

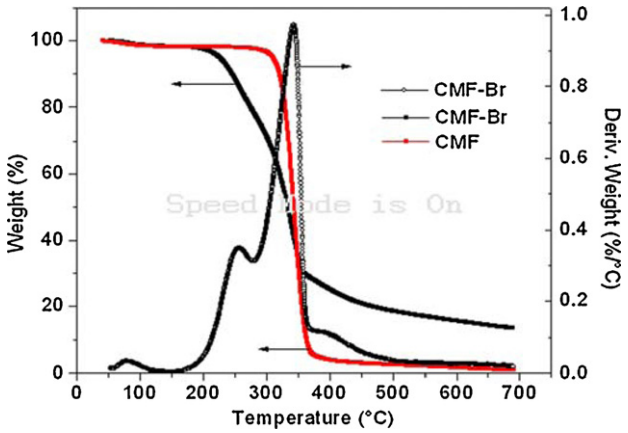


**Fig. 3.** TG and DTG curves of CMF and CMF-Br.

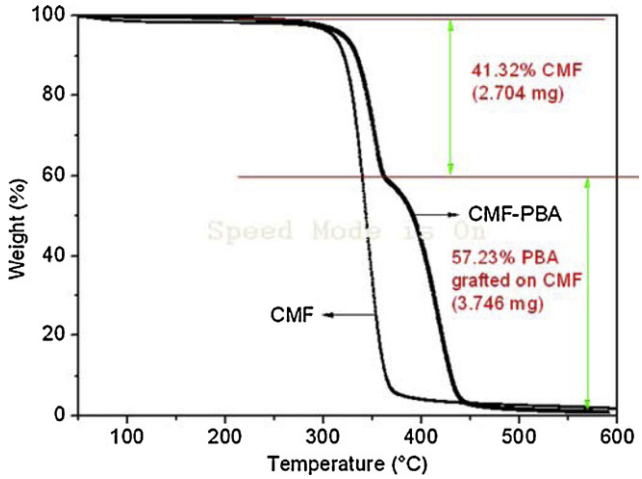


**Fig. 4.** TG curves of CMF and CMF-PBA.

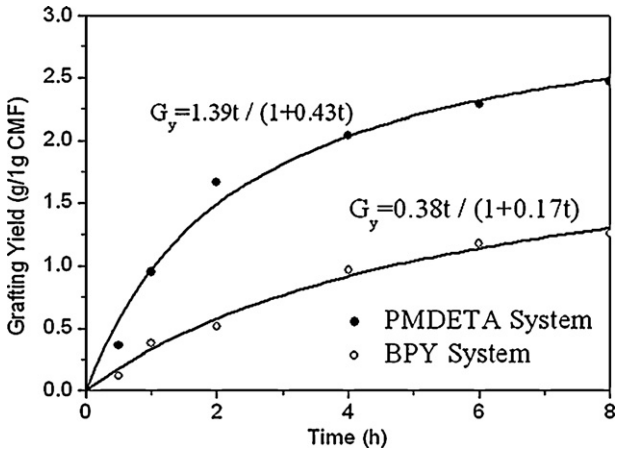


**Fig. 5.** Grafting yield of BA vs. time for ATRP initiated by CMF-Br with PMDETA system and BPY system in DMF at 90 °C [Br (in CMF-Br)]/[CuIBr]/[PMDETA]/[BA] = 1:1:1:39, [Br (in CMF-Br)]/[CuIBr]/[BPY]/[BA] = 1:1:3:39.

sistent with those reported elsewhere (Peter, Bernard, & Bohuslav, 2000). Therefore, the thermal stability of CMF-Br is lower than that of original CMF. It is worth mentioning that if the first smaller decomposition peak at 230 °C resulted from the degradation of BIBB, the amount of BIBB in CMF-Br would be 11.7% (wt.) from the calculation of the weight loss from the calculation of the weight loss from 150 °C to 275 °C in the TGA curves in Fig. 3. Correspondingly, the molar amount of Br on 1 g CMF-Br would be $0.8 \times 10^{-3}$ mol, which enabled us to select an appropriate amount of monomers for targeted MW.

### 3.2. Kinetics of the ATRP of butyl acrylate initiated by CMF-Br with $Cu^{I}Br$/PMDETA and $Cu^{I}Br$/BPY catalyst systems

With the CMF-Br macromolecular initiator prepared above, SI-ATRP polymerization of BA was carried out in DMF solvent at 90 °C under nitrogen, using either $Cu^{I}Br$/PMDETA or $Cu^{I}Br$/BPY as catalyst system. The grafting yield is determined according to the weight loss obtained from TGA analysis, which is similar to a thermal-gravimetric method reported elsewhere (El-Khouly et al., 2010).

Fig. 4 shows the TGA curves of unmodified CMF and grafted CMF. For CMF-PBA TGA curves, the initial weight loss around 300 °C represents the degradation of CMF, which is in correspondence with tTGA curve of CMF. The weight percent of CMF based on the total weight ($W_{CMF}$) can be directly obtained using the TGA software (TA universal analysis). The second weight loss around 400 °C indicates the degradation of PBA grafted onto the CMF. The weight percent of PBA ($W_{PBA}$) can also be obtained with the TGA software. As a result, the grafting yield ($G_y$) can be estimated from the ratio of the second weight loss ($W_{PBA}$ = 57.23 wt.%) to the first weight loss ($W_{CMF}$ = 41.32 wt.%), which is 1.39. The plots of the grafting yield of polymerization as a function of reaction time for both catalyst systems are shown in Fig. 5. The nonlinearity of the relation between grafting yield and reaction time implies the loss of some bromine elements on CMF-Br during the course of polymerization. It should be noted that the surface-initiated ATRP systems are heterogeneous, which deviates from homogeneous ATRP systems in terms of polymerization kinetics due to the complex side-reactions. The leveling-off of grafting yield might be attributed to the polymerization occurring in bulk phase, i.e., in the solution instead of the surface of CMF, induced by chain transfer or thermal-induced radicals in the solution. The polymerization in the bulk phase could cause either a drop in monomer concentration or the fouling of the surface. The deviation from linear curve of the grafting yield could also be due to the termination from radical combination on the surface of CMF.

To further ascertain the side-reactions that led to the leveling-off of the grafting yield, the reaction mixture was filtered, and the solution of the CMF suspension was collected and analyzed by $^{1}H$ NMR. However, the result did not show the presence of polymers in the solution. Therefore, this can neglect possible contributions to the leveling-off from surface fouling or chain transfer reactions, such as radical transfer to solution or monomers. Accordingly, the combination termination reactions on the surface of CMF appear to be the key reasons for the leveling-off of grafting yield vs. time.

To further determine the characteristics of PBA chains grafted on CMF via SI-ATRP using PMDETA catalyst system, the cleaving-off of the polymer grafts was performed via hydrolysis. As described above, the grafts, PBA, were also hydrolyzed to PAA after the hydrolysis. Since the hydrolyzed polymers were fully water soluble, it was confirmed that PBA grafts were all hydrolyzed to be PAA. Therefore, the GPC results of the cleaved-off polymers from CMF-PBA are attributed to PAA. The molecular weight of PBA could be calculated from the degree of polymerization (DP) of PAA, which is the same as that of PBA. The polydispersity of PAA could directly represent that of PBA as well. As shown in Fig. 6, the GPC results indicated bi-model peaks and broad molecular weight distribution. The first weak peak, corresponding to the high retention volume (i.e., long retention time), suggested that a small portion of PBA formed had relatively high molecular weight. This implies that the combination termination might occur throughout the polymerization. The second sharp peak indicated that the majority of BA monomers were grafted onto the surface of the CMF via SI-ATRP, leading to

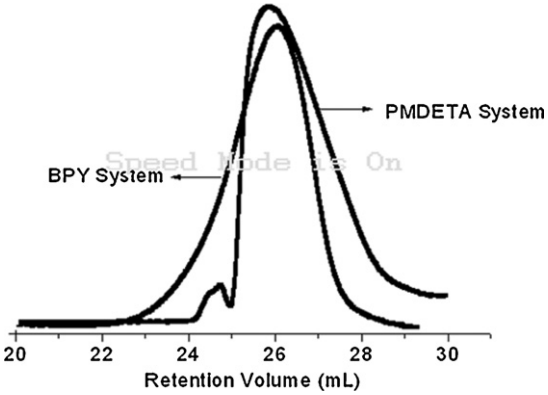


**Fig. 6.** GPC traces of the polymers cleaved-off from CMF-PBA samples prepared using PMDETA system and BPY system.

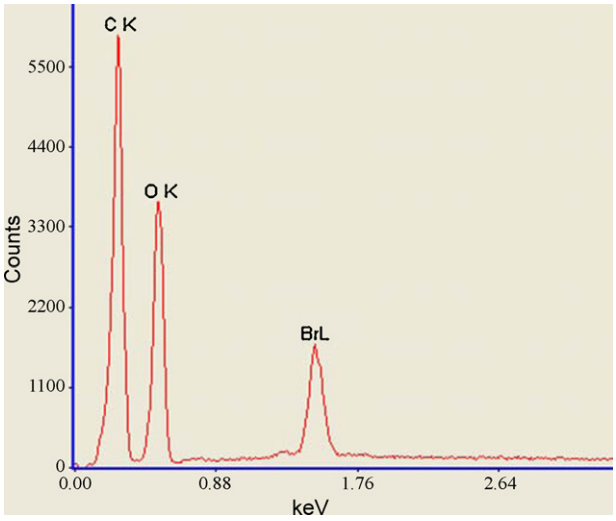


**Fig. 7.** EDAX spectra of CMF-PBA.

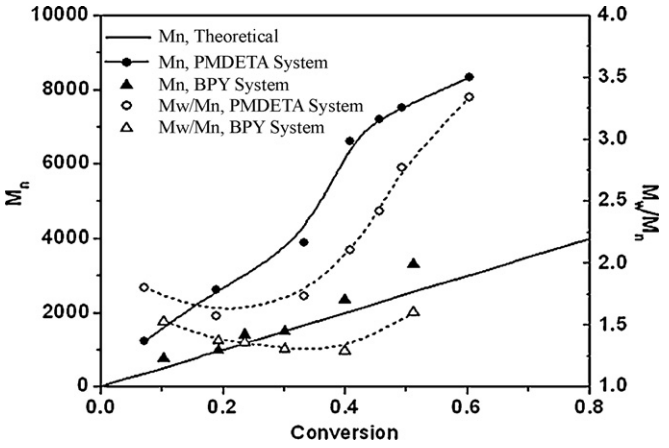


**Fig. 8.** Dependence of molecular weight, $M_n$, and polydispersity, $M_w/M_n$, on monomer conversion for the ATRP of butyl acrylate initiated by CMF-Br with a PMDETA system and BPY system in DMF at 90 °C for 24 h.

the grafted polymers with relatively broad MWD. Moreover, the tailing for low MW, shown in Fig. 6, for PMDETA system suggested the presence of oligomer chains on the surface of CMF. This could be attributed either to the bromine atoms becoming steric inaccessible after being buried in the PBA film or to the loss of bromine from the PBA chains. As PMDETA was used when BPY was used as a ligand, however, only the tailing corresponding to high MW was observed (Fig. 6, BPY system). The tailing at shorter retention time and the its absence at longer retention time suggested that the combination termination indeed occurred and the steric inaccessibility of bromine atoms was negligible due to the slower polymerization rate throughout the reaction.

Overall, the level-off of the grafting yield in the current systems appears to be unavoidable due to the combination termination likely occurring throughout the polymerization. The radical combination is a particular concern for surface polymerization as it often leads to a surface for which the reactive groups are in close proximity. Since the propagation rate is linear in $[R^\bullet]$ but the termination rate is proportional to $[R^\bullet]^2$, the controlled growth of polymer from surface can be achieved by reducing the radical concentration (Xiao & Wirth, 2002).

To investigate the accessibility of bromine atoms on the surface of the CMF-PBA produced by PMDETA system, EDAX was used to probe the presence of bromine atoms. Fig. 7 shows the EDAX spectra of CMF-PBA prepared in PMDETA system. The peak of Br was clearly observed around 1.48 keV in Fig. 7, indicating the polymerization is still "living" in spite of the loss of a small portion of Br over the reaction.

Assuming there is only combination termination for SI-ATRP, a kinetic model for the surface polymerization using ATRP has been reported (Xiao & Wirth, 2002). Consequently, the conversion of polymerization has simple nonlinear time dependence:

$$\frac{[M]_0 - [M]}{[M]_0} = \frac{k_p[R^\bullet]_0 t}{1 + [R^\bullet]_0 k_t t} \quad (2)$$

Since the grafting yield ($G_y$) is proportional to $[M]_0 - [M]$, the continuous curves presented in Fig. 5, which well fit the experimental data for both ligand systems, provided important kinetic data for the purpose of comparison.

In terms of the results or parameters of fitting the curve in Fig. 5, it is clear that the propagation rate for the PMDETA system, $[M]_0 k_p [R^\bullet]_0$, is 3.6-fold faster than that for BPY system; and the termination rate, $[R^\bullet]_0\ k_t$, is 2.5-fold faster. Therefore, the results elucidated the reason why the final grafting yield in PMDETA system was higher. The dependence of the number-average molecular weight ($M_n$) and polydispersity ($M_w/M_n$) on the monomer conversion (up to 24 h reaction time), estimated from Eq. (2), for both PMDETA and BPY systems is shown in Fig. 7. An approximately linear increase of $M_n$ versus monomer conversion was found for the BPY system. The observed $M_n$ and theoretical values based on $\Delta[M]/[I]_0$ was well matched, even though the measured $M_n$ deviated from the theoretical one at the late stage of the reaction or high conversion due to the combination termination. The result also suggested that an insignificant degree of transfer occurred during the polymerization. The molecular weight distribution decreased as the reaction proceeded, becoming relatively narrow, $M_w/M_n < 1.3$ until 40% monomer conversion and then increased.

Conversely, the MW of the polymers produced in PMDETA system was not well controlled. As can be seen from Fig. 8, the $M_n$ values obtained were much higher than the predicted or theoretical values. The polydispersities were much broader with the $M_w/M_n > 3.0$ in the late stage of the polymerization. The increase in polydispersity is thought to be caused by the combination termination because the polymerization rate in this system was very fast, in which almost 50% of monomers were consumed in 4 h, however the reaction mixture was kept reacting for 24 h, leading to more combination termination reactions.

### 3.3. *Effect of various solvents on the SI-ATRP of butyl acrylate on CMF*

For the $Cu^IBr$/BPY system, the polymerization rate was slow, and the grafting yield appeared to be limited as shown in Fig. 5. On the other hand, $Cu^IBr$/BPY creates a heterogeneous system in most solvents due to the poor solubility of BPY, which tends to lead to uncontrollable polymerization. In contrast, the polymerization of BA with $Cu^IBr$/PMDETA appeared to be faster but generated the polymers with broad MW distribution. In an attempt to achieve the better control of MW and polydispersity of the grafted PBA on CMF produced in $Cu^IBr$/PMDETA system, several solvents, including DMF, toluene and 1-butanol, were used in the ATRP of butyl acrylate at 90 °C, with the monomer concentration fixed at 20% (w/w). The effect of the solvent on the grafting yield is presented in Fig. 9.

As can be seen from Fig. 9, the grafting yield increased with the increase of the reaction time, and meanwhile, the solvents indeed affected the polymerization and termination rate strongly. The polymerization rate in DMF is 1.7 times faster than that in toluene and 5 times faster than that in butanol. On the other hand, the termination rate in DMF is the fastest among three sol-

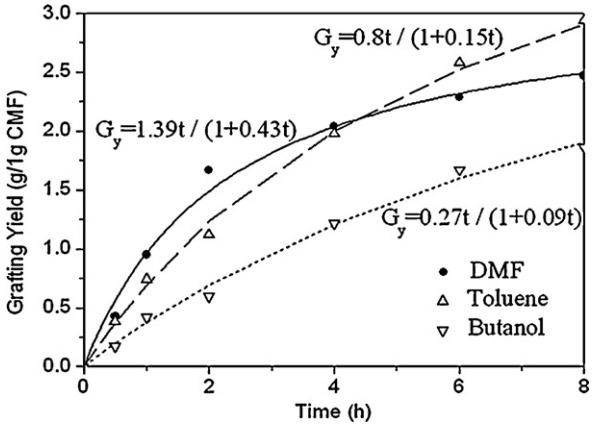


**Fig. 9.** Grafting yield vs. time for ATRP initiated by CMF-Br with a PMDETA system in DMF, toluene and 1-butanol at 90 °C [Br (in CMF-Br)]/[CuIBr]/[PMDETA]/[BA] = 1:1:1:39.

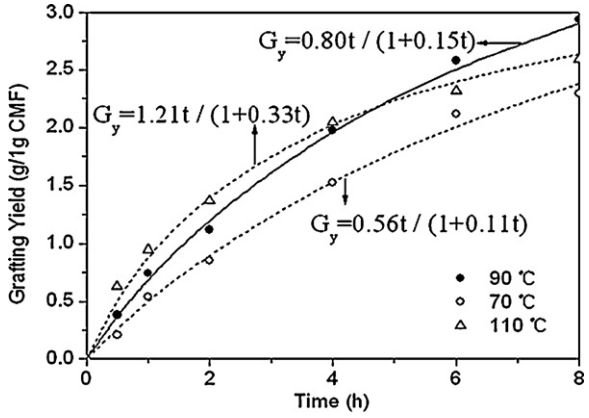


**Fig. 11.** Grafting yield of BA vs. time for ATRP initiated by CMF-Br with a PMDETA system in toluene at 90 °C, 70 °C and 110 °C, [Br (in CMF-Br)]/[CuIBr]/[PMDETA]/[BA] = 1:1:1:39.

vents, 2.9 times faster than that in toluene and 4.8 times faster than that in butanol. The results are consistent with the findings on the effect of solvents on the ATRP of BA catalyzed by CuBr/N-(*n*-hexyl)-2-pyridylmethanimine (Zhang & Rob, 2002). The faster polymerization in DMF may be due to the high polarity of DMF (Chambard, Klumperman, & German, 2000). The high polarity of solvent tends to promote the activation of macroinitiator (Chambard et al., 2000), thus increasing the concentration of radicals; but meanwhile leading to a high rate of termination. The decrease in the polymerization rate in 1-butanol is probably due to the presence of large self-regulation at the beginning of the reaction, which produced a high Cu(II) concentration and, therefore, slowed down the reaction (Fischer, 1997), In addition, for the current reaction system the poor dispersity of macroinitiator, CMF-Br, in 1-butanol further decreased the polymerization rate. The lower termination reaction rate for 1-butanol is also attributed to its higher viscosity. As the termination reaction is diffusion-controlled, the higher viscosity of the 1-butanol solvent is expected to lower $k_t$ (Kurenkov & Myagchenkov, 1980; North & Reed, 1961).

Fig. 10 shows the effects of the solvents on the molecular weights and MW distributions. For the ATRP systems in toluene and 1-butanol, $M_n$ increased linearly with increasing monomer conversion and was very close to the theoretical values. However, $M_n$ values were higher than the predicted ones in DMF, and the deviation from the theoretical value became even profound at the conversion of BA above 40%, implying the inefficient initiation and the presence of the coupling termination reaction.

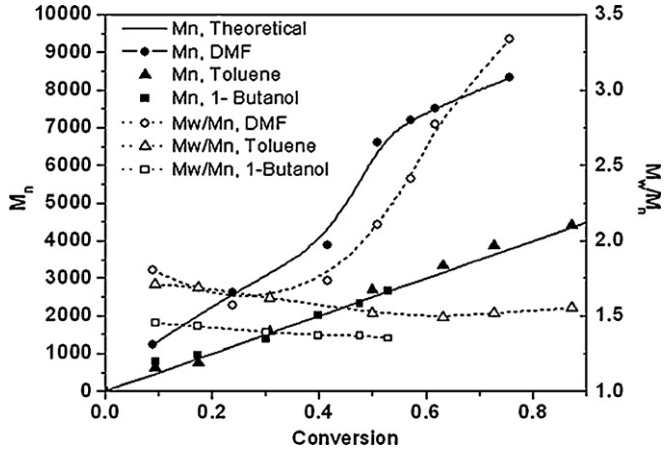


**Fig. 10.** Effect of solvents on the molecular weight, $M_n$, and polydispersity, $M_w/M_n$ as a function of monomer conversion for the ATRP of butyl acrylate initiated by CMF-Br with PMDETA system; ATRP was conducted at 90 °C with a monomer concentration fixed at 20% (w/w).

A significant difference was also observed in the polydispersity of the polymers prepared in different solvents (Fig. 10). 1-Butanol and toluene, 1-butanol in particular, led to the polymers with relatively low polydispersities; and $M_w/M_n$ could be as low as 1.3. The narrow MW distribution in 1-butanol might be attributed to the high activation rate constant of ATRP, which tends to generate to a high ratio of the initiation rate to the propagation rate, thereby reducing the polydispersity values. The polymerization rates and conversion of BA in 1-butanol, however, were much lower than those in toluene and DMF. In the case of DMF, the polydispersity increased with the conversion, which might be caused by combination termination reaction and steric inaccessibility of bromine atoms. The rapid growth of PBA chains on the surface of CMF-Br could bury part of Br on the surface, thus becoming inactive.

On the basis of these results, the SI-ATRP of butyl acrylate on CMF with $Cu^{I}Br$/PMDETA in toluene was considered to be an appropriate system for further studies, giving a moderate polymerization rate and relatively good control of molecular weight. Therefore, toluene was used as the solvent in the following studies.

### 3.4. Effect of the reaction temperature on the polymerization

The effect of the reaction temperature on the polymerization was studied over a temperature range of 70–110 °C (Fig. 11). As can be seen, the reaction temperature has a positive effect on the polymerization rate, as should be expected. However, an increased termination reaction at a high temperature (i.e., 110 °C) was observed. According to the parameters in the fitting curves, the polymerization rate at 110 °C was doubled, compared with that at 70 °C; whereas the termination rate was almost tripled at the elevated temperature, thereby lowering the grafting yield. The increase of polymerization rate with temperature is due to the increase of both the radical propagation rate constant and the atom transfer equilibrium constant. As a result of the higher activation energy for the radical propagation than that for the radical termination, the higher $k_p/k_t$ ratios would be expected at a high temperature (Matyjaszewski & Xia, 2001). However, the chain transfer and other side-reactions become profound at elevated temperatures (Matyjaszewski, 1998; Matyjaszewski, Davis, Patten, & Wei, 1997), implying the intensified termination reactions.

Fig. 12 presents the effect of the reaction temperature on the MW and MW distributions. The experimental molecular weights increased linearly with increasing monomer conversion and were close to the theoretical values at 70 °C and 90 °C, but slightly

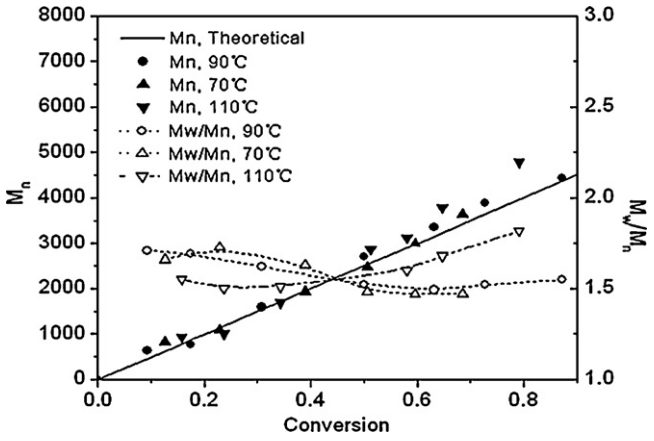


**Fig. 12.** Dependence of molecular weight, $M_n$, and polydispersity, $M_w/M_n$, on monomer conversion for the ATRP of butyl acrylate initiated by CMF-Br with a PMDETA system in toluene at 90 °C, 70 °C and 110 °C.

deviated at a high conversion at 110 °C. Similarly, the elevated temperature (i.e., 110 °C) led to the polymers with a relatively broader MW than those at low reaction temperatures.

### 3.5. Effect of deactivator $Cu^{II}Br_2$ on the polymerization

In fact, at a high monomer conversion, the polymerization rate is slowed down considerably; however, the rate of any side reaction does not change significantly, which tends to be independent of monomer concentration (Matyjaszewski & Xia, 2001). Moreover, it has been reported that the broadening of MWDs is probably due to the fact that thermal acceleration is greater for propagation than for the interconversion rate between the dormant and the activated species with temperature (Hiroko, Yuzo, Masami, & Mitsuo, 1998). Therefore, in our reaction systems, the reaction at 90 °C appears to give the best results in terms of the polymerization rates and MW distributions.

In ATRP, the presence of an X-$Cu^{II}$/ligand complex is necessary to reduce the concentration of radicals through a deactivation process in order to maintain the activation–deactivation equilibrium for the controlled growth of the polymer chains with conversion (Fischer, 1999; Kajiwara, Matyjaszewski, & Kamachi, 1998; Matyjaszewski, Ajaya, & Tang, 2005). To reduce the polydispersities, the addition of Cu(II) to the reaction mixture was employed in the earlier study (Matyjaszewski, Yoshiki, & Christina, 1998). In the present work, 5% (mol) of $Cu^{II}Br_2$ relative to $Cu^{I}Br$ was added at the beginning of polymerization for the purpose of further optimizing the controllable polymerization. Surprisingly, the polymerization rate decreased drastically instead of increasing. Only 20% of monomer conversion was achieved within a reasonable polymerization period (24 h). The observed $M_n$ was also close to the theoretical values throughout the reaction; and the polydispersities decreased to $M_w/M_n \leq 1.19$. It has been found that due to radical confinement the irreversible termination reactions might be fast, leading to an increase in the deactivator concentration [Cu(II) complex] in the medium and then shifting in the activation–deactivation equilibrium, thereby favoring the formation of dormant species (Carrot et al., 2001). Therefore, the addition of Cu(II) at the beginning of the reaction further restrained the formation of active species, allowing the polymerization controllable at a low concentration of radicals.

## 4. Conclusions

The SI-ATRP of butyl acrylate was successfully conducted on the surface of CMF, thus leading to the hydrophobic-modified CMF with tailored soft corona suitable for a verity of potential applications. CMF-Br macroinitiator was obtained by esterification of OH groups on CMF with 2-bromoisobutyryl bromide. The presence of bromine atoms was verified by FT-IR and EDAX; whereas the amount of Br on the surface was quantified using TGA. Such Br concentration provided a basis for predetermining the arm chain length of PBA.

ATRP of butyl acrylate using BPY in DMF produced the PBA with well-defined and desirable structures, i.e., controllable MW and low polydispersities; but meanwhile retarded polymerization rate. In contrast, PMDETA system in DMF led to a rapid polymerization but deteriorated the control over MW and polydispersities. To optimize the polymerization using the $Cu^{I}Br$/PMDETA system, different solvents were employed and assessed. It was found that toluene provided better control of MW and polydispersities, compared with other solvents. In addition, the reaction temperature had a profound effect on the polymerization rate and the polydispersity of grafted PBA. The use of $Cu^{II}Br_2$ as a co-catalyst improved the polydispersity but decreased the monomer conversion. The CMF modified with SI-ATRP of BA is a promising reinforcement for biocomposites.

## Acknowledgements

The NSERC Canada, Auto 21 NCE and NSERC Green Wood Fibre Network are gratefully acknowledged for financial support.

## References

Amash, A., & Zugenmaier, P. (1998). Study on cellulose and xylan filled polypropylene composites. *Polymer Bulletin*, *40*, 251–258.
Anna, C., & Eva, E. M. (2003). ATRP grafting from cellulose fibers to create block-copolymer grafts. *Biomacromolecules*, *4*, 1740–1745.
Belgacem, M. N., & Gandini, A. (2005). The surface modification of cellulose fibres for use as reinforcing elements in composite materials. *Composite Interfaces*, *12*, 41–75.
Carlmark, A., & Malmstrom, E. (2003). ATRP grafting from cellulose fibers to create block-copolymer grafts. *Biomacromolecules*, *4*, 1740–1745.
Carrot, G., Diamanti, S., Manuszak, M., Charleux, B., & Vairon, J. P. (2001). Atom transfer radical polymerization of n-butyl acrylate from silica nanoparticles. *Journal of Polymer Science Part A: Polymer Chemistry*, *39*, 4294–4301.
Castellano, M., Gandini, A., Fabbri, P., & Belgacem, M. N. (2004). Modification of cellulose fibres with organosilanes: Under what conditions does coupling occur? *Journal of Colloid and Interface Science*, *273*, 505–511.
Chambard, G., Klumperman, B., & German, A. L. (2000). Effect of solvent on the activation rate parameters for polystyrene and poly(butyl acrylate) macroinitiators in atom transfer radical polymerization. *Macromolecules*, *33*, 4417–4421.
Coskun, M., & Temüz, M. M. (2005). Grafting studies onto cellulose by atom-transfer radical polymerization. *Polymer International*, *54*, 342–347.
David, P., Katja, J., Helge, E., & Søren, H. (2005). Modification of jute fibers with polystyrene via atom transfer radical polymerization. *Biomacromolecules*, *75*, 2474–2484.
Dufresne, A., Cavaille, J. Y., & Helbert, W. (1996). New nanocomposite materials: Microcrystalline starch reinforced thermoplastic. *Macromolecules*, *29*, 7624–7626.
El-Khouly, A. S., Takahashi, Y., Takada, A., Safaan, A. A., Kenawy, E., & Hafiz, Y. A. (2010). Characterization and thermal stability of cellulose-graft-polyacryloniytrile prepared by using $KMnO_4$/citric acid redox system. *Journal of Applied Polymer Science*, *116*, 1788–1795.
Ejaz, M., Tsujii, Y., & Fukuda, T. (2001). Controlled grafting of a well-defined polymer on a porous glass filter by surface-initiated atom transfer radical polymerization. *Polymer*, *42*, 6811–6815.
Favier, V., Chanzy, H., & Cavaille, J. Y. (1995). Polymer nanocomposites reinforced by cellulose whiskers. *Macromolecules*, *28*, 6365–6367.
Fischer, H. (1997). The persistent radical effect in "living" radical polymerization. *Macromolecules*, *30*, 5666–5672.
Fischer, H. (1999). The persistent radical effect in controlled radical polymerizations. *Journal of Polymer Science Part A: Polymer Chemistry*, *37*, 1885–1901.
Gaelle, M., Lindy, H., & Wim, T. (2009). Cellulose nanocrystals grafted with polystyrene chains through surface-initiated atom transfer radical polymerization (SI-ATRP). *Langmuir*, *25*, 8280–8286.
Glaied, O., Dubé, M., Chabot, B., & Daneault, C. (2009). Synthesis of cationic polymer-grafted cellulose by aqueous ATRP. *Journal of Colloid and Interface Science*, *333*, 145–151.
Grassie, N., & MacFarlane, I. G. (1978). The thermal degradation of polysiloxanes—I. Poly(dimethylsiloxane). *European Polymer Journal*, *14*, 875–884.
Grassie, N., Murry, E. J., & Holmes, P. A. (1984). The thermal degradation of poly(-(D)-β-hydroxybutyric acid): Part 2—Changes in molecular weight. *Polymer Degradation and Stability*, *6*, 95–103.

Gupta, K. C., & Sahoo, S. (2001). Graft copolymerization of acrylonitrile and ethyl methacrylate comonomers on cellulose using ceric lons. *Biomacromolecules*, *2*, 239–247.

Hiroko, U., Yuzo, K., Masami, K., & Mitsuo, S. (1998). $NiBr_2(Pn\text{-}Bu_3)_2$-mediated living radical polymerization of methacrylates and acrylates and their block or random copolymerizations. *Macromolecules*, *31*, 6756–6761.

Josefina, L., Daniel, N., Emma, O., Per, A., Anna, C., Mats, J., et al. (2008). Intelligent dual-responsive cellulose surfaces via surface-initiated ATRP. *Biomacromolecules*, *9*, 2139–2145.

Josefina, L., & Eva, M. (2006). Surface modification of natural substrates by atom transfer radical polymerization. *Journal of Applied Polymer Science*, *100*, 4155–4162.

Kajiwara, A., Matyjaszewski, K., & Kamachi, M. (1998). Simultaneous EPR and kinetic study of styrene atom transfer radical polymerization (ATRP). *Macromolecules*, *31*, 5695–5701.

Kalaprasad, G. N., & Alain, D. (2003). Crab shell chitin whisker reinforced natural rubber nanocomposites. 2. Mechanical behavior. *Biomacromolecules*, *4*, 1835–1842.

Koening, S. H., & Roberts, C. W. (1974). Vinybenzyl ethers of cellulose. Preparation and polymerization. *Journal of Applied Polymer Science*, *18*, 651–666.

Kong, H., Gao, C., & Yan, D. Y. (2004). Controlled functionalization of multiwalled carbon nanotubes by in situ atom transfer radical polymerization. *Journal of the American Chemical Society*, *126*, 412–413.

Kong, X. X., Tadashi, K., Jiro, A., & Tomokazu, I. (2001). Amphiphilic polymer brushes grown from the silicon surface by atom transfer radical polymerization. *Macromolecules*, *34*, 1837–1844.

Kurenkov, V. F., & Myagchenkov, V. A. (1980). Effects of reaction medium on the radical polymerization and copolymerization of acrylamide. *European Polymer Journal*, *16*, 1229–1239.

Li, D. X., He, Q., Cui, Y., & Li, J. B. (2007). Fabrication of pH-responsive nanocomposites of gold nanoparticles/poly(4-vinylpyridine). *Chemistry of Materials*, *19*, 412–417.

Liu, P., & Guo, J. S. (2006). Polyacrylamide grafted attapulgite (PAM-ATP) via surface-initiated atom transfer radical polymerization (SI-ATRP) for removal of Hg(II) ion and dyes. *Colloids and Surfaces A: Physicochemical and Engineering Aspects*, *282–283*, 498–503.

Marutani, E., Yamamoto, S., Ninjbadgar, T., Tsujii, Y., Fukuda, T., & Takano, M. (2004). Surface-initiated atom transfer radical polymerization of methyl methacrylate on magnetite nanoparticles. *Polymer*, *45*, 2231–2235.

Matyjaszewski, K. (1998). Transformation of "living" carbocationic and other polymerizations to controlled "living" radical polymerization. *Macromolecular Symposium*, *134*, 105–118.

Matyjaszewski, K., Ajaya, K. N., & Tang, W. (2005). Effect of $[Cu^{II}]$ on the rate of activation in aTRP. *Macromolecules*, *38*, 2015–2018.

Matyjaszewski, K., Davis, K., Patten, T., & Wei, M. (1997). Observation and analysis of a slow termination process in the atom transfer radical polymerization of styrene. *Tetrahedron*, *53*, 15321–15329.

Matyjaszewski, K., Miller, P. J., Shukla, N., Immarporn, B., et al. (1999). Polymers at interfaces: Using atom transfer radical polymerization in the controlled growth of homopolymers and block copolymers from silicon surfaces in the absence of untethered sacrificial initiator. *Macromolecules*, *32*, 8716–8724.

Matyjaszewski, K., & Xia, J. H. (2001). Atom transfer radical polymerization. *Chemical Reviews*, *101*, 2921–2990.

Matyjaszewski, K., Yoshiki, N., & Christina, B. J. (1998). Polymerization of n-butyl acrylate by atom transfer radical polymerization. Remarkable effect of ethylene carbonate and other solvents. *Macromolecules*, *31*, 1535–1541.

Mohamed, E. M., Mostafa, M., & Alain, D. (2005). Thermoplastic nanocomposites based on cellulose microfibrils from Opuntia ficus-indica parenchyma cell. *Composites Science and Technology*, *65*, 1520–1526.

North, A. M., & Reed, G. A. (1961). Diffusion-controlled termination during the initial stages of free radical polymerization of methyl methacrylate. *Transactions of the Faraday Society*, *57*, 859–870.

Otto van den, B., Michael, S., Jeffrey, R. C., & Christoph, W. (2007). Nanocomposites based on cellulose whiskers and (semi)conducting conjugated polymers. *Journal of Materials Chemistry*, *17*, 2746–2753.

Peter, J., Bernard, R., & Bohuslav, V. K. (2000). Thermal degradation behavior of cellulose fibers partially esterified with some long chain organic acids. *Polymer Degradation and Stability*, *70*, 387–394.

Plackett, D., Jankova, K., Egsgaard, H., & Hvilsted, S. (2005). Modification of jute fibers with polystyrene via atom transfer radical polymerization. *Biomacromolecules*, *6*, 2474–2484.

Pyun, J., Kowalewski, T., & Matyjaszewski, K. (2003). Synthesis of polymer brushes using atom transfer radical polymerization. *Macromolecular Rapid Communications*, *24*, 1043–1059.

Robert, W., Anna, C., Anders, H., Eva, M., & Isabel, M. S. (2007). Grafting liquid crystalline polymers from cellulose substrates using atom transfer radical polymerization. *Soft Matter*, *3*, 866–871.

Sang, Y. Z., & Xiao, H. N. (2009). Preparation and application of cationic cellulose fibers modified by in situ grafting of cationic PVA. *Colloids and Surfaces A: Physicochemical and Engineering Aspects*, *335*, 121–127.

Shah, R. R., Merreceyes, D., Husemann, M., Rees, I., Abbott, N. L., Hawker, C. J., et al. (2000). Using atom transfer radical polymerization to amplify monolayers of initiators patterned by microcontact printing into polymer brushes for pattern transfer. *Macromolecules*, *33*, 597–605.

Singh, N., Chen, Z., Tomer, N., Wickramasinghe, S. R., Soice, N., & Husson, S. M. (2008). Modification of regenerated cellulose ultrafiltration membranes by surface-initiated atom transfer radical polymerization. *Journal of Membrane Science*, *311*, 225–234.

Uchida, E., & Ikada, Y. (1997). Topography of polymer chains grafted on a polymer surface underwater. *Macromolecules*, *30*, 5464–5469.

Valter, C., Marco, G., Simone, G., & Giulia, M. (2007). Cotton fibers encapsulated with homo- and block copolymers: synthesis by the atom transfer radical polymerization grafting-from technique and solid-state NMR dynamic investigations. *Biomacromolecules*, *8*, 498–508.

Vigo, T. L. (1998). Intelligent fibrous substrates with thermal and dimensional memories. *Polymers for Advanced Technologies*, *9*, 539–548.

William, J. O., Justin, S., Syed, H. I., Gregory, M. G., Mara, E. G., & Jean-Francois, R. J. (2005). Application of cellulose microfibrils in polymer nanocomposites. *Journal of Polymers and the Environment*, *13*, 301–306.

Xiao, D. Q., & Wirth, M. J. (2002). Kinetics of surface-initiated atom transfer radical polymerization of acrylamide on silica. *Macromolecules*, *35*, 2919–2925.

Zadorecki, P., & Ronnhult, T. (1986). Esca study of chemical reactions on the surfaces of cellulose fibers. *Journal of Polymer Science Part A: Polymer Chemistry*, *24*, 737–745.

Zampano, G., Bertoldo, M., Bronco, S., & Simona, B. (2009). Poly(ethyl acrylate) surface-initiated ATRP grafting from wood pulp cellulose fibers. *Carbohydrate Polymers*, *75*, 22–31.

Zhang, H. Q., & Rob, V. D. L. (2002). Atom transfer radical polymerization of n-butyl acrylate catalyzed by CuBr/N-(n-hexyl)-2-pyridylmethanimine. *Journal of Polymer Science Part A: Polymer Chemistry*, *40*, 3549–3561.

Zhang, L., & Chen, L. (2002). Water-soluble grafted polysaccharides containing sulfobetaine groups: Synthesis and characterization of graft copolymers of hydroxyethyl cellulose with 3-dimethyl(methacryloyloxyethyl)ammonium propane sulfonate. *Journal of Applied Polymer Science*, *83*, 2755–2761.

Zhao, B., & Brittain, W. J. (1999). Synthesis of tethered polystyrene-block-poly(methyl methacrylate) monolayer on a silicate substrate by sequential carbocationic polymerization and atom transfer radical polymerization. *Journal of the American Chemical Society*, *121*, 3557–3558.